Hindawi Publishing Corporation
Advances in Materials Science and Engineering
Volume 2013, Article ID 382534, 8 pages
http://dx.doi.org/10.1155/2013/382534

Research Article

Contribution of Process Annealing on the Development of Microstructure and Texture of Cu-30Zn Brass

S. Hagos,[1] A. K. Verma,[2] Prantik Mukhopadhyay,[3] and A. K. Singh[3]

[1] *Defence Institute of Advanced Technology, Pune 411025, India*
[2] *SSQAG, c/o ASL Laboratory, Hyderabad 500058, India*
[3] *Defence Metallurgical Research Laboratory, Hyderabad 500058, India*

Correspondence should be addressed to Prantik Mukhopadhyay; prantikmukherje@gmail.com

Received 20 May 2013; Revised 6 August 2013; Accepted 20 August 2013

Academic Editor: Aloysius Soon

The present study describes the development of microstructural and textural trends with and without process annealing of the Cu-30Zn brass. Process-annealing refines the grain size and randomizes the crystallographic texture. The best benefits of grain refinement and randomization of texture have been obtained in process-annealing after early stage of deformation. The crucial advantages of (random + Bs) texture strengths in formability of final cold rolled gauges and annealed sheets have also been highlighted.

1. Introduction

Advanced fabrication of cartridge brass incorporates drawing at room temperature in several stages with intermittent process-annealing, which induces ductility to enhance the further deep drawing [1]. The refinement of grain size [2] conventionally increases the total ductility and toughness, while random texture brings isotropic properties [3]. The development of deformation texture of fcc metals and alloys has shown two distinct textural trends, Cu{112}⟨111⟩ and Bs{110}⟨112⟩ texture [4–6]. The lower strain produces nonuniform dislocation distribution, while deformation at higher degree develops deformation heterogeneities [7–10] like transition band, shear band, and twins. Deformation character based on the very low stacking fault energy (SFE) of cartridge brass has been described elsewhere [11]. The developments of solely Bs texture and Cu to Bs deformation texture transition harboured by earlier research [12] have been projected contradiction by recent report [13]. The predominant crystallographic recrystallization texture is developed in the annealing temperature range (550–650°C) [14]. The recrystallization texture after hot rolling of brass is governed by rolling texture [15]. The SEM-EBSD has revealed the occurrence of nucleation from deformation heterogeneity and preferred growth of certain grain boundaries [16] in copper single crystal, lightly annealed after compression.

Cold drawing of cartridge brass enhances the hardness in the actual practice, but the same level of hardness can also be obtained by 50% cold rolling of this alloy [1]. Hence, the deformation scenario by deep drawing might be approximated by rolling. Cold drawing produces earing problem due to Cube annealing texture and cold rolling texture components in high SFE fcc alloys [17]. Elimination of the forming related problem requires the isotropic forming [18] properties. An attempt has, therefore, been made in present study to randomize the texture of finally cold rolled and annealed Cu-30Zn brass in order to obtain the possible benefits of isotropic properties in formability.

2. Materials and Methods

The minute details of process annealing technique are represented in Figure 1. The hot rolled (HR) 0.0035 meter thick Cu-30Zn brass sheet was processed by three routes (no. 1 to no. 3). In no. 1, hot rolled sheet was first cold rolled to 14% (true strain $\varepsilon = 0.15$) then interannealed at 575°C for 10 minutes followed by cold rolling to total 30% ($\varepsilon = 0.35$) and

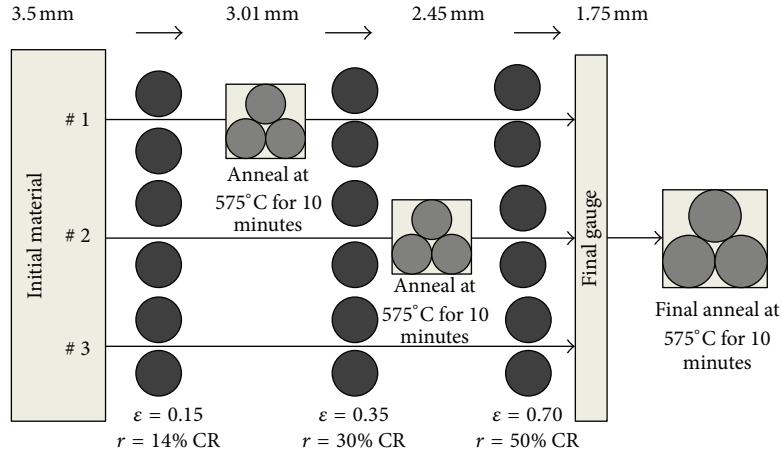

Figure 1: Sheet fabrication with and without process-annealing.

total 50% ($\varepsilon = 0.70$) reductions. The final annealed sheet (L1) was obtained from annealing of 50% cold rolled (R1) gauge at 575°C for 10 minutes. In no. 2, hot rolled sheet was first cold rolled to 14% and then total 30% reduction followed by interannealing at 575°C for 10 minutes. The annealed sheet was further cold rolled to gauge with total 50% reduction (R2) and then finally annealed (L2). The cold rolling of hot rolled sheet was performed without interannealing in no. 3, where hot rolled sheet was first cold rolled to total 50%, and the rolled gauge (R3) was annealed at similar annealing condition to obtain the finally annealed sheet (L3).

Samples for optical microscopy were prepared using standard metallographic technique. The mean grain size ($\overline{L}$) and grain size distribution (% number frequency with $L\,\mu$m) were measured with Sigma-scanPro-5 software by line intercept method in the rolling direction. The {111}, {200}, {220}, and {311} pole figures were measured by X-ray texture Goniometer. The prominent ideal orientations were selected from orientation distribution functions (ODF) plots, and then the texture strength of ideal orientation was derived surrounding the ideal orientation with the angular spread 5° by LaboTex-Edu software. The texture trend is represented by texture strength of ideal (T_i) and random ($100 - \sum T_i$) orientations.

3. Results and Discussion

The mean grain size ($\overline{L}$) and grain size distribution of as received (HR), 50% cold rolled gauges (R1, R2, and R3), and final annealed sheets (L1, L2, and L3) are shown in Figure 2. The contribution of interannealing on refinement of microstructure is shown in Figure 2(a). The average grain size gradually increases from R1 to R3. The inter-annealing (no. 1 and no. 2) refines the microstructure of 50% cold rolled gauge. An early interannealing is required with respect to cold rolling reduction to get the highest level of grain size refinement of cold rolled gauge. Further refinement of microstructures in (L1, L2, and L3) samples is associated with an annealing treatment of R1, R2, and R3 samples. An interannealing treatment at the early stage (no. 1 after 14% cold rolling degree) produces the maximum grain refinement (L1) while that has insignificant contribution in controlling grain size (L2) when performed at later stage of cold rolling (no. 2 after 30% cold reduction).

Table 1: Representation of ideal texture orientations.

Orientation	Notation
Cube	{001}⟨100⟩
Brass (Bs)	{110}⟨112⟩
Cu	{112}⟨111⟩
R	{123}⟨412⟩
S	{123}⟨643⟩
Goss (G)	{110}⟨001⟩
Taylor	{4411}⟨11118⟩
H	{001}⟨110⟩
CG	{021}⟨100⟩
CH	{001}⟨120⟩
L	{011}⟨522⟩
Z	{113}⟨332⟩
C	{236}⟨385⟩

HR sample shows a log-normal distribution, while the R1 sample is associated with highest population of refined grains (Figure 2(b)) and displays bimodality in distribution. The R2 sample possesses a balanced number frequency of coarse and refined grains, while the R3 sample adheres to higher frequency of larger grains. The grain size distributions of (L1-L2) samples show the trend of near log-normal distribution with the higher population of finer grains for L1 and L2 samples, while L3 sample reveals bimodality in grain size distribution (Figure 2(c)).

Figure 3 deals with the ODF plots of HR, R1, R2, and R3 samples, and Figure 4 illustrates the ODF plots of L1, L2, and L3 samples. The locations of ideal texture components with their crystallographic indices are displayed in Figure 4(d) and Table 1. The ODF plot of HR sample is associated with randomized Cube texture with traces of Bs, Cu, and S

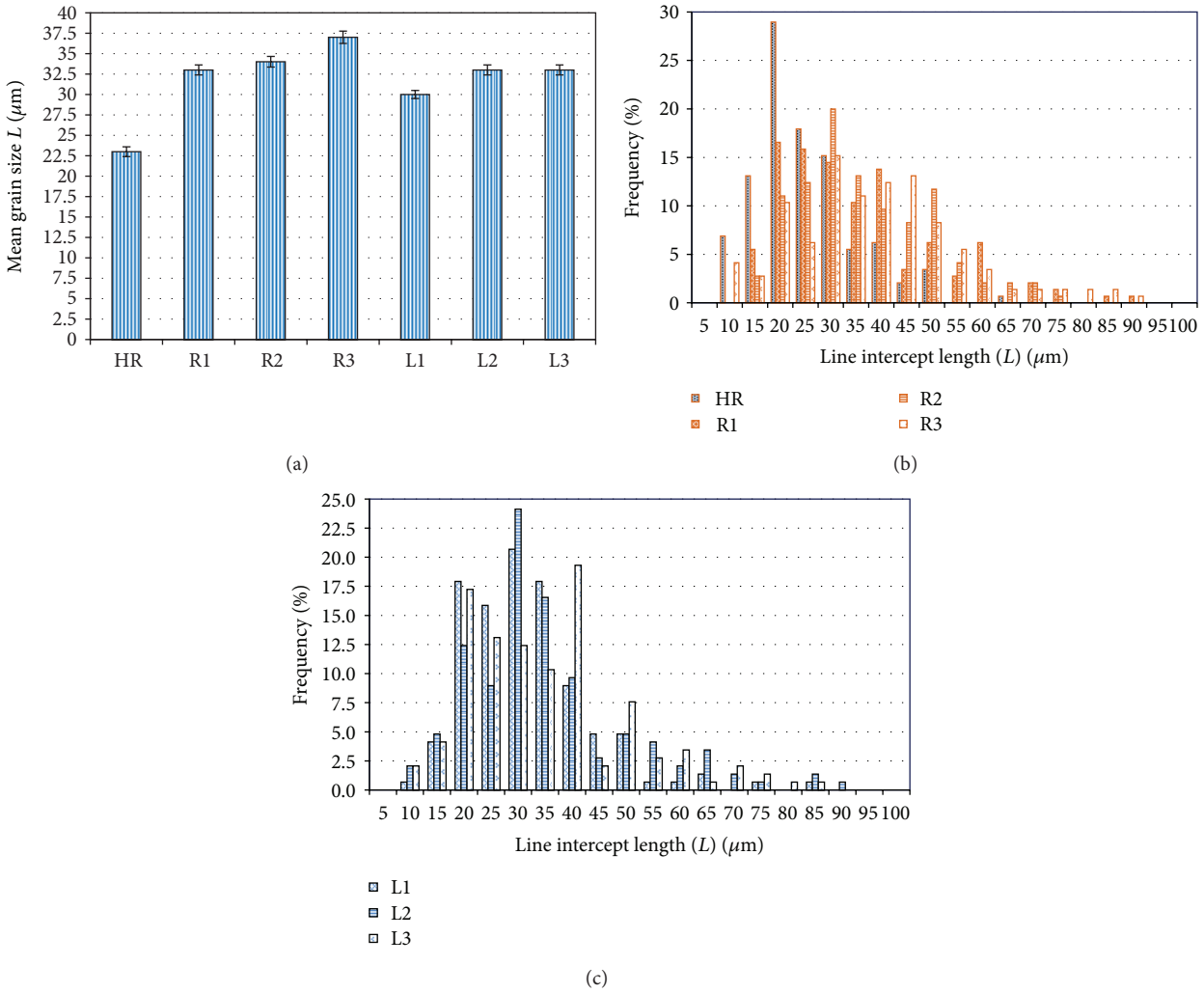

FIGURE 2: (a) Mean grain size of as received, final cold rolled, and annealed samples. (b) Grain size (L) distribution of final cold rolled samples. (c) Grain size (L) distribution of final annealed samples.

components. The comparative analysis of the ODFs of HR, R1, R2, and R3 samples shows that the HR is adhered to higher intensities of Cube, rotated Cube orientations (CG, H, and CH) and lower intensities of Bs, Cu, and S components than those of the R1, R2, and R3 samples (Figure 3). The higher intensity of Cu, and S orientations has been found in R3 than R1 and R2 samples, but Bs component shows just opposite trend, with highest intensity in R1 sample. Figure 4 delineates the randomized intensities of annealing texture of L1 and L2 samples than L3 sample. The intensities of rolling texture components decrease, while the intensities associated with Cube and rotated Cube orientations (CG, H, and CH) increase than those of the R1, R2, and R3 samples. The significant contribution of annealing is prominent in L1 sample in the randomization of Bs component. The salient strengths of ideal texture orientations of final rolled gauge and final annealed gauge are shown in Figures 5(a) and 5(b), respectively, and further, the associated random (random + Bs) texture strengths are delineated in Figure 6. Several ideal texture orientations have been observed in ODF plots with significant higher intensities than random texture. The texture strengths (% volume fraction) of all these ideal texture orientations were derived and deducted from 100 to obtain the degree (% volume fraction) of randomness in totality. This has not been properly pointed out by the highest intensity of orientation distribution function plots. Table 2 describes the textural trends obtained from R1, R2, and R3 samples, and Table 3 emphasizes the final annealing textural trend of L1, L2, and L3 samples (Figure 5). The texture developments of 50% cold rolled gauges (Figure 5(a)) show that the strength of ideal texture components like Cube, CG, G, and Bs decreases but the strengths of R, C, and S components increase from R1 to R3. Cold rolled R3 sample reveals the highest strength of Cu, Taylor (T), and Z orientations, while R1 and R2 show constant but less strength. The strengths of H and CH orientations do not vary in R2 and R3 samples and are less than that of the R1. The strength of the L orientation obtained from R1 increases in R2 and then decreases in R3.

The texture strengths of Cube, L, and Bs orientations after annealing (Figure 5(b)) of cold rolled gauge gradually

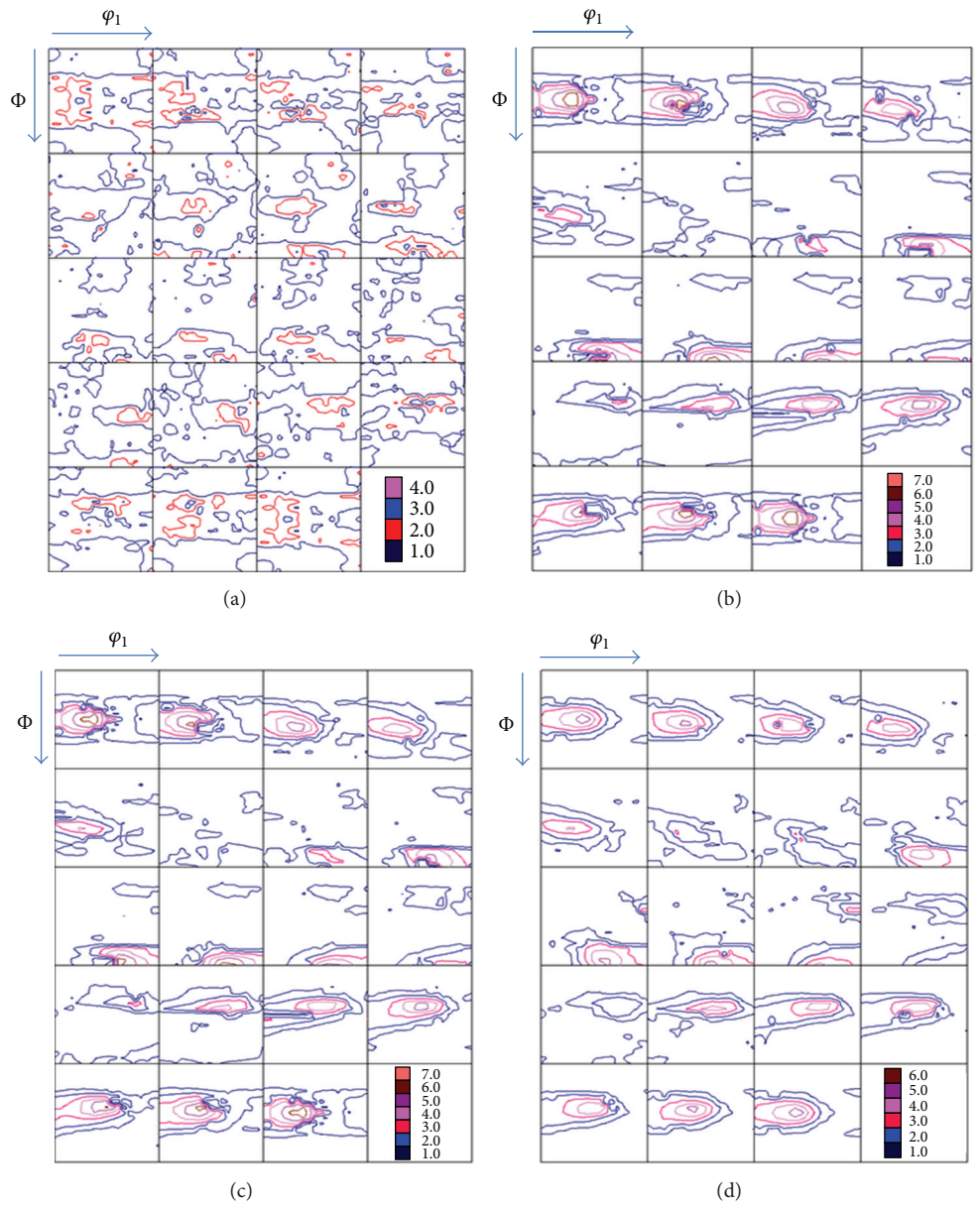

Figure 3: (a) Orientation distribution function (constant φ_2 sections) of hot rolled sample. (b) Orientation distribution function (constant φ_2 sections) of R1 sample. (c) Orientation distribution function (constant φ_2 sections) of R2 sample. (d) Orientation distribution function (constant φ_2 sections) of R3 sample.

Table 2: Texture trend of final cold rolled gauge (from R1 to R3).

Texture orientation	Texture trend
Cube, Bs, G, CG	Strength gradually decreases from R1 to R3.
S, R, C	Strength gradually increases from R1 to R3.
Cu, Taylor, Z	Strengths constant in R1 and R2 with the increase in R3.
H, CH	Highest strength in R1 and decrease and constant in R2 and R3.
L	First increases and then decreases. Highest strength in R2

increase, but R components decrease from L1 to L3. The strengths of CG and S components obtained from L1 increase in L2 and then decrease in L3. The texture strengths of Cu, T, and Z do not vary in L2 and L3 samples and are less than that of the L1. The strengths of G, H, CH, and C components obtained from L1 decrease slightly in L2 and then increase in L3.

The present process annealing reveals, namely, grain refinement and randomization of texture which have significant bearing on forming properties required for adequate formability [18]. These properties are (i) high plastic anisotropic parameter (R) value with proper texture,

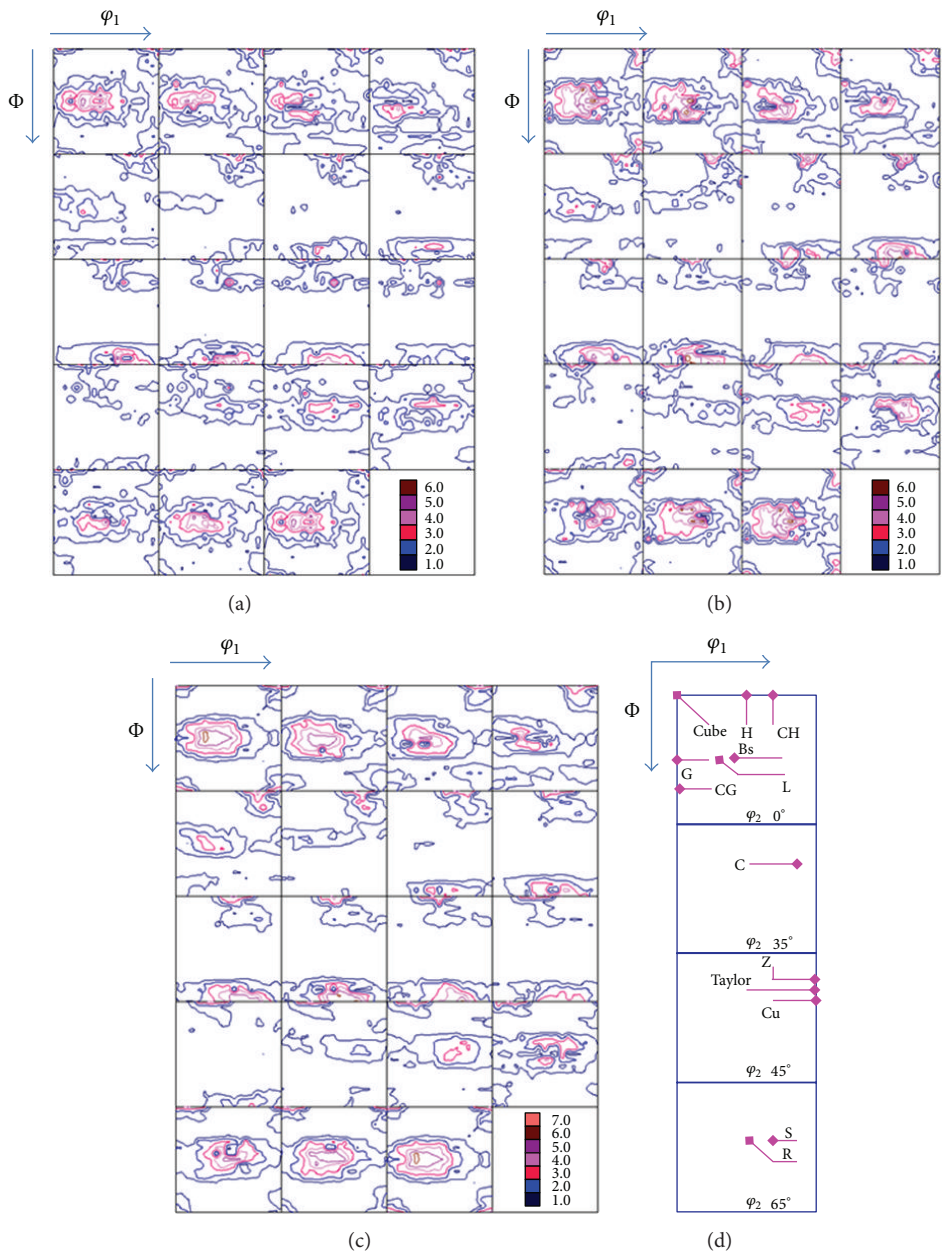

FIGURE 4: (a) Orientation distribution function (constant φ_2 sections) of L1 sample. (b) Orientation distribution function (constant φ_2 sections) of L2 sample. (c) Orientation distribution function (constant φ_2 sections) of L3 sample. (d) Ideal orientation locations at constant φ_2 sections 0°, 35°, 45°, and 65°.

(ii) high work hardening exponent, (iii) high uniform and total ductility, and (iv) low yield strength and low rate of strain ageing.

The refinement of grain size with least concentration of interstitial elements of the Cu-30Zn brass reduces the pronounced yield point and strain aging problems during forming [2]. The higher the work hardening exponent, the greater is the work hardening rate and the higher the uniform ductility [2]. The very low SFE of Cu-30Zn brass and associated difficulty in cross slip delay the dynamic softening during forming and result in high uniform strain with greater work hardening exponent. The refinement of grain size also plays significant role in work hardening. The greater degree of refinement increases the work hardening rate but it also increases the yield stress. The degree of contributions in these factors might be identical. Hence grain refinement has no effect on uniform ductility, but it yields higher total ductility [18]. The process annealing refines the grain size of both (R1, R2) and L1 samples. It is best suited at early stage (R1 and L1) after 14% cold rolling than after 30% cold rolling (R2 and L2).

The microstructure of HR sample is adhered to a log-normal grain size distribution. The bimodality of R1 sample

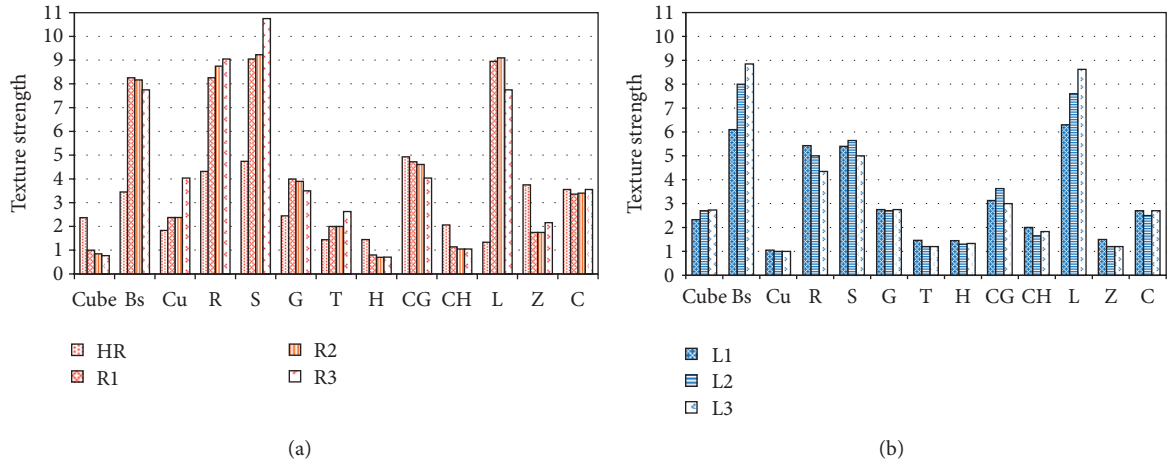

Figure 5: (a) Texture strength of ideal texture components after final cold rolling. (b) Texture strength of ideal texture components after final annealing.

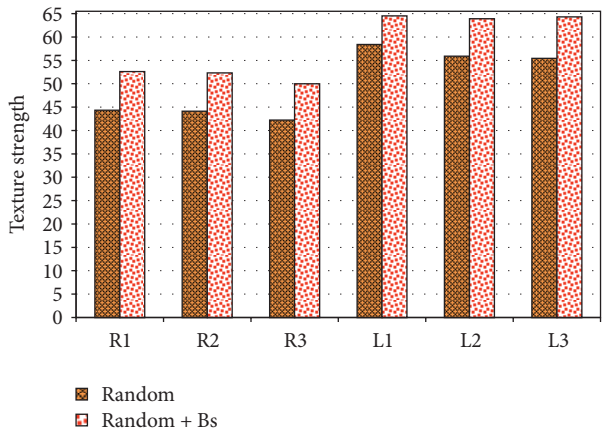

Figure 6: Texture strength of random (random + Bs) texture component.

Table 3: Texture trend of final annealed gauge (from L1 to L3).

Texture orientation	Texture trend
Cube, L, Bs	Strength gradually increases from L1 to L3.
R	Highest strength in L1. Lowest strength without process annealing.
S, CG	First increase then decrease. Highest strength in L2.
Cu, Taylor, Z	Highest strength in L1 and decease and constant in L2 and L3.
G, H, CH, C	Highest strength in L1, decreases in L2, and then increases in L3.

is addressed by the selective elongation of softer grains with deformation. The bimodal grain size distribution of R1 sample became log-normal distribution with higher population of finer grains in L1 sample. This is attributed to 50% cold rolling of 14% cold rolled and annealed sample which has accumulated enough elastic energy of dislocations for developing fine recrystallized grains after final annealing.

It is known that the combinations of larger and finer grains result in multimodality in grain size distribution [19]. The finer grains yield high uniform ductility and work hardening rate, while coarse grains reduce yield strength. A combination of these effects brings some benefit in formability but the definite advantage, in crucial issues of formability, lies with the contribution of both the grain size as well as texture. The high plastic anisotropic parameter values of low carbon mild steel which are beneficial for adequate formability are associated with larger grain size and {111} or Cube on corner preferred orientation [18]. The larger size {111} oriented grains are formed due to oriented growth driven by higher mobility of grain boundaries. Unlike steel, the pronounced deformation and annealing textures of Cu-30Zn brass are not of type {111} or Cube on corner type. Although the presence of the Y{111}⟨112⟩ component in fcc alloys is reported [5, 10, 12, 20], but this is not the prominent texture orientation in present study. The characteristic Cube texture with remnants of rolling texture is observed after annealing of high SFE fcc alloys, while Bs with components of grain growth are reported to be associated with annealing texture of low SFE fcc alloys [21]. The planar anisotropy derived from deformation and annealing texture of high SFE fcc alloys shows that the Cube component and also deformation texture components are harmful for earing which occurs with certain angular deviations [17]. Therefore, the benefits of isotropic properties are required to control the planar anisotropy near zero, randomising the deformation and recrystallization texture in order to eliminate the earing problem of these alloys [17].

The microstructure of HR sample is adhered to randomized Cube texture and traces of rolling texture components. The dramatic change of HR texture is associated with deformation by rolling, where shear components (Cu, Bs, Goss, and S) and associated Cube grain rotation develop

rolling textures [12, 13]. The highest strengths of Cube, CG, G, CH, H, and Bs are associated with R1 sample. The G and Bs orientations are seen to be developed with deformation, strengthening the α-fibre. The development of Bs orientation is observed to be preferred by both deformation and annealing. The strengthening of Bs, S, Cu, L, R, T, and G components compared to hot rolled (HR) texture in R3 samples undoubtedly reveals the deformation induced selective developments. The strength of L orientation in the α-fibre increases with interannealing with its highest strength in R2 sample. The degree of textural randomization obtained in R1 and R2 is higher than that of the R3 sample. Annealing produces separate trend of textural development. The selective development of Cube, Bs, CH, and H is observed (no. 3) in annealing presumably by discontinuous recrystallization due to very low SFE. The L1 sample is associated with lowest strength of Cube and Bs and highest strength of Cu, T, Z, R, G, C, CH, and H orientations. The less strength of Cube and Bs in L1 compared to texturing by Cu, G, C, CH, and H components resulted in the randomization of texture which is also observed in L2 with comparatively less degree. The R1, L1, R2, and L2 samples show the higher degree of randomization in totality. The degree of randomization is benefited by process-annealing and is best suited when process-annealing is performed after an early stage of cold rolling. The sequence of getting higher isotropic properties during forming of Cu-30Zn brass for finally rolled and annealed samples, therefore, will be R3-R2-R1 and L3-L2-L1, respectively. The formability of Cu-30Zn brass is often determined by Bs annealing texture supplemented by grain growth components [21]. Hence, the presence of Bs orientation in randomized texture will definitely bring the dual benefit in forming by both the random texture and Bs component with high strength in the R1 and L1 samples.

4. Conclusions

Process-annealing at the early stage of deformation introduces grain size refinement and randomness of texture of final 50% rolled gauges and annealed sheets. It results in best benefits when process annealing is carried out after 14% than that of after 30% cold rolled conditions.

Conflict of Interests

None of the authors have direct financial relation with commercial identities like Sigma-ScanPro5 and Labotex-Edu software.

Acknowledgments

The authors would like to thank Dr. A. A. Gokhale Director DMRL for constant encouragement. The research grant of Defence Institute of Advanced Technology, Pune, is acknowledged to carry out this work.

References

[1] A. Doig, *Military Metallurgy*, Maney, London, UK, 1998.

[2] V. Raghavan, *Physical Metallurgy, Principles and Practice*, Prentice Hall Private Limited, New Delhi, India, 2nd edition, 2006.

[3] G. E. Dieter, *Mechanical Metallurgy*, McGraw-Hill, London, UK, 1988.

[4] S. Pasebani, M. R. Toroghinejad, M. Hosseini, and J. Szpunar, "Textural evolution of nano-grained 70/30 brass produced by accumulative roll-bonding," *Materials Science and Engineering A*, vol. 527, no. 7-8, pp. 2050–2056, 2010.

[5] M. Salari and A. Akbarzadeh, "Effect of microstructural inhomogeneities on texture evolution in 90–10 Brass sheets," *Journal of Materials Processing Technology*, vol. 182, no. 1–3, pp. 440–444, 2007.

[6] M. Miraglia, P. Dawson, and T. Leffers, "On the influence of mechanical environment on the emergence of brass textures in FCC metals," *Acta Materialia*, vol. 55, no. 3, pp. 799–812, 2007.

[7] R. L. Fleischer, "Number of active slip systems in polycrystalline brass: implications for ductility in other structures," *Acta Metallurgica*, vol. 35, no. 8, pp. 2129–2136, 1987.

[8] W. Y. Yeung and B. J. Duggan, "On the plastic strain carried by shear bands in cold-rolled α-brass," *Scripta Metallurgica*, vol. 21, no. 4, pp. 485–490, 1987.

[9] B. Gonzalez, L. E. Murr, O. L. Valerio, E. V. Esquivel, and H. Lopez, "Microbands and microtwins associated with impact craters in copper and brass targets: the role of stacking fault energy," *Materials Characterization*, vol. 49, no. 4, pp. 359–366, 2003.

[10] J. Hirsch, K. Lücke, and M. Hatherly, "Overview No. 76: mechanism of deformation and development of rolling textures in polycrystalline f.c.c. metals-III. The influence of slip inhomogeneities and twinning," *Acta Metallurgica*, vol. 36, no. 11, pp. 2905–2927, 1988.

[11] F. J. Humphreys and M. Hatherly, *Recrystallization and Related Annealing Phenomena*, Elsevier, Oxford, UK, 2004.

[12] J. Hirsch and K. Lücke, "Overview no. 76: mechanism of deformation and development of rolling textures in polycrystalline f.c.c. metals-I. Description of rolling texture development in homogeneous CuZn alloys," *Acta Metallurgica*, vol. 36, no. 11, pp. 2863–2882, 1988.

[13] T. Leffers and R. K. Ray, "The brass-type texture and its deviation from the copper-type texture," *Progress in Materials Science*, vol. 54, no. 3, pp. 351–396, 2009.

[14] K. Lücke and U. Schmidt, "The recrystallization texture of α-brass," *Journal of the Less Common Metals*, vol. 28, no. 1, pp. 187–191, 1972.

[15] M. Hatherly, A. S. Malin, C. M. Carmichael, F. J. Humphreys, and J. Hirsch, "Deformation processes in hot worked copper and α brass," *Acta Metallurgica*, vol. 34, no. 11, pp. 2247–2257, 1986.

[16] H. Paul, J. H. Driver, C. Maurice, and Z. Jasieński, "Crystallographic aspects of the early stages of recrystallisation in brass-type shear bands," *Acta Materialia*, vol. 50, no. 17, pp. 4339–4355, 2002.

[17] J. Liu, S. W. Banovic, R. J. Fields, and J. G. Morris, "Effect of intermediate heat treatment on microstructure and texture evolution of continuous cast Al-Mn-Mg alloy sheet," *Metallurgical and Materials Transactions A*, vol. 37, no. 6, pp. 1887–1891, 2006.

[18] F. B. Pickering, *Physical Metallurgy and the Design of Steels*, Applied Science Publisher Limited, London, UK, 1978.

[19] K. S. Suresh, S. Sinha, A. Chaudhary, and S. Suwas, "Development of microstructure and texture in Copper during warm accumulative roll bonding," *Materials Characterization*, vol. 70, pp. 74–82, 2012.

[20] E. El-Danaf, S. R. Kalidindi, R. D. Doherty, and C. Necker, "Deformation texture transition in brass: critical role of micro-scale shear bands," *Acta Materialia*, vol. 48, no. 10, pp. 2665–2673, 2000.

[21] T. Oeztuerk and G. J. Davies, "Texture and formability in fcc metals and alloys," *Material Science and Technology*, vol. 5, no. 2, pp. 186–193, 1989.